

PUBLISHED BY

# INTECH

open science | open minds

World's largest Science,  
Technology & Medicine  
Open Access book publisher



**3,150+**  
OPEN ACCESS BOOKS



**104,000+**  
INTERNATIONAL  
AUTHORS AND EDITORS



**109+ MILLION**  
DOWNLOADS



**BOOKS**  
DELIVERED TO  
151 COUNTRIES

AUTHORS AMONG

**TOP 1%**  
MOST CITED SCIENTIST



**12.2%**  
AUTHORS AND EDITORS  
FROM TOP 500 UNIVERSITIES



Selection of our books indexed in the  
Book Citation Index in Web of Science™  
Core Collection (BKCI)

**WEB OF SCIENCE™**

Chapter from the book *Ultra-Wideband Radio Technologies for Communications, Localization and Sensor Applications*

Downloaded from: <http://www.intechopen.com/books/ultra-wideband-radio-technologies-for-communications-localization-and-sensor-applications>

Interested in publishing with InTechOpen?  
Contact us at [book.department@intechopen.com](mailto:book.department@intechopen.com)

---

# Power Allocation Procedure for Wireless Sensor Networks with Integrated Ultra-Wide Bandwidth Communications and Radar Capabilities

---

Gholamreza Alirezaei, Rudolf Mathar and Daniel Bielefeld

Additional information is available at the end of the chapter

<http://dx.doi.org/10.5772/53005>

---

## 1. Introduction

In this chapter, we analyze the problem of power allocation for a distributed wireless sensor network with sensor nodes based entirely on ultra-wide bandwidth (UWB) technology. The network is used to perform object detection as well as object classification, where the absence, the presence, or the type of an object is observed by the sensors independently. UWB signals can be used for data communication between the sensor nodes as well as for radar applications. The approach of misemploying the communication sensors as radar sensors, such that the data transmission is misused as a radar beam in order to detect or to classify a target object, helps in realizing an energy-efficient radar system with compact and cheap sensor nodes. A further advantage of such radar systems is the fulfillment of major requirements of wireless sensor networks. This exploitation presupposes that the integration of sensing functionality into usual UWB sensors is implementable easily without the usage of any additional hardware units. Since the compact and low complexity UWB sensors are limited in power and communication capabilities, the detection and classification performance of a single sensor is restricted compared to that of a common complex radar system. To obtain an appropriate overall system performance, we consider the case of distributed detection and classification, where the local observations of the sensors are fused into a reliable global decision. Due to noisy communication channels and differences in distances between the object and the sensor nodes, both, the observations and their transmissions are unequally interfered. One simple way to suppress noise interference is to increase the power of each sensor node. But if the total power of the entire network is limited, then power allocation procedures are needed in order to increase the overall detection and classification probabilities. In general, it is challenging to evaluate the detection and the classification probabilities analytically, if possible at all. This particularly holds for the detection probability under a Neyman-Pearson-hypotheses-test criterion as well as for the classification probability under a Bayesian-hypotheses-test criterion [5]. This limits the usability of these criteria for analytical optimization of power allocation. Bounds, such as the Bhattacharyya bound [8], are also difficult to use for optimizing multidimensional

problems. Therefore, we employ an information theoretic approaches [3], which help to solve the power allocation problem with a lower mathematical complexity. This approach yields a simple however suboptimal analytical solution for the power allocation problem. Furthermore, the proposed technique enables the consideration of object detection and classification at the same time. This is a further advantage of this method, which enables the usage of the same allocation algorithm in both cases. Hence a sensor network, which is used to classify target objects, can also be used to detect the absence or the presence of a target object with equal system settings. Therefore we only describe the case of object classification, which also includes the case of object detection, in the following sections.

The origin of research on distributed detection has been the attempt to fuse signals of different radar devices [10]. Currently, distributed detection is usually discussed in the context of wireless sensor networks, where the sensor unit of the nodes might be based on radar technology [7, 9, 14]. Other applications for UWB radar systems, which require or benefit from the detection and classification capabilities, are for example localization and tracking [6] or through-wall surveillance [4]. The physical layer design for an integrated UWB radar network that utilizes OFDM technology was analyzed in [11]. In [2] the case of object detection is considered, where for the problem of power allocation an approach based on the maximization of the Kullback-Leibler distance is used. In a recent publication [1] another approach is discussed, where the bit-error probability of data communication is used in order to allocate the transmission power and to increase the overall detection probability.

This chapter is divided into the following three sections except the introduction. First, the system model of the wireless network including sensor nodes and the fusion center is described. Here, all system parameters and assumptions with detailed mathematical formulations are introduced. Furthermore, the global classification rule in the fusion center as well as the local decision rules in the nodes are motivated. In the second section, we present a novel approach for power allocation in order to increase the overall classification probability, following which, the solution of this optimization approach is briefly discussed. The last section shows some results and demonstrates the feasibility of object classification by using the proposed power allocation method in UWB signaling systems. This chapter concludes with an interpretation of the achieved system performance.

## 2. System model

Throughout this chapter we denote the set of natural, real, and complex numbers by  $\mathbb{N}$ ,  $\mathbb{R}$ , and  $\mathbb{C}$ , respectively. Note that the set of natural numbers does not include the element zero. Furthermore, we use the subset  $\mathbb{F}_N \subseteq \mathbb{N}$  which is defined as  $\mathbb{F}_N := \{1, \dots, N\}$  for any given natural number  $N$ . The mathematical operations  $|z|$  and  $\|\mathbf{z}\|$  denote the absolute value of a real or complex-valued number  $z$  and the Euclidian length of a real or complex vector  $\mathbf{z}$ , respectively.

Distributed *target object* classification can be formally modeled by a multiple hypotheses testing problem with hypotheses  $H_k \forall k \in \mathbb{F}_K$  for a specified number  $K \in \mathbb{N}$  of different objects. We assume that all objects have the same size, shape, alignment, and position. They only differ in material and are classified by their complex-valued reflection coefficients  $r_k \in \mathbb{C}$ , which are ordered in a strictly increasing manner  $0 \leq |r_1| < \dots < |r_K| \leq 1$ . Therefore the reflection coefficients are the only recognition features in this work. Generally, this assumption is not realistic, but, this case describes an ideal scenario for increasing the classification probability by performing a power allocation and is not really suitable for analyzing the problems of manifoldness.

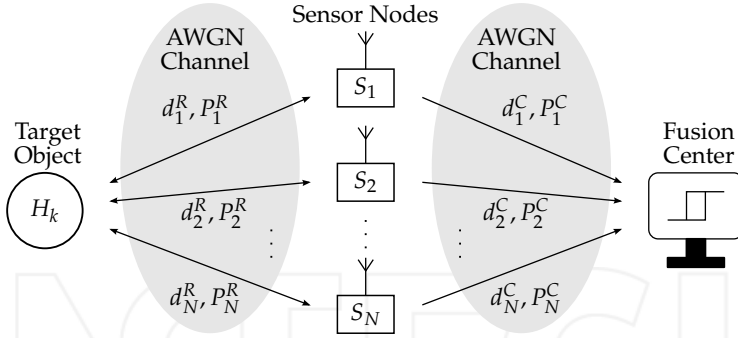


**Figure 1.** System model of the distributed wireless sensor network.

At any instance of time, a network of  $N \in \mathbb{N}$  independent and spatially distributed sensors, as shown in Figure 1, obtains random observations  $X_1, \dots, X_N \in \mathbb{R}$ . In the case of energy classification,  $X_n$  models the received signal at the receiver of the  $n^{\text{th}}$  sensor. If a target object is present, then the received energy is a part of the radiated energy of the same sensor, which is reflected from the object's surface and is weighted by its reflection coefficient. We refer to this communication channel, between the sensors and the target object, as the *first* communication link and denote all dedicated parameters by the superscript  $R$ . The random observations  $X_1, \dots, X_N$  are assumed to be conditionally independent for each of the underlying hypotheses, i.e., the joint conditional probability density function of all the observations factorizes according to

$$f^R(X | H_k) := \prod_{n=1}^N f_n^R(X_n | H_k), \quad \forall k \in \mathbb{F}_K, \quad (1)$$

where  $X$  denotes the sequence of random variables  $X_1, \dots, X_N$ . In general, the observations are not identically distributed because the sensor nodes have different distances  $d_n^R$  from the target object and their radiated powers  $P_n^R$  are also different. Therefore, the signal-to-noise ratio (SNR) varies between the sensor nodes. Due to the distributed nature of the problem, the  $n^{\text{th}}$  sensor  $S_n$  performs independent measurements and processes its respective observation  $X_n$  by generating a local decision  $U_n := \theta_n(X_n) \forall n \in \mathbb{F}_N$ , which depends only on its own observation and not on the observations of other sensor nodes. After deciding locally, each sensor transmits its decision to a fusion center located at a remote location. The communication between the sensor node and the fusion center is determined by the corresponding distance  $d_n^C$  as well as by the transmission power  $P_n^C$  of the same sensor node. We refer to this communication channel, between the sensor nodes and the fusion center, as the *second* communication link and denote all dedicated parameters by the superscript  $C$ . Furthermore, we assume that both communication channels are non-fading channels and that all data transmissions are affected only by additive white Gaussian noise (AWGN). We disregard time delays within all transmissions and assume synchronized data communication. We use two distinct pulse-shift patterns for each sensor node in order to distinguish its first and second communication link from the communication links of other sensor nodes as described in [13]. Each pattern has to be suitably chosen in order to suppress inter-user interference at each receiver. Hence the  $N$  received signals at the fusion center are uncorrelated and are assumed to be conditionally independent for each of the underlying hypotheses. These received random signals correspond to the local decisions  $U_1, \dots, U_N$  and

are mapped to  $\tilde{\mathbf{X}}_1, \dots, \tilde{\mathbf{X}}_N \in \mathbb{R}^K$ . Their joint conditional probability density function factorizes according to

$$f^C(\tilde{\mathbf{X}} | H_k) := \prod_{n=1}^N f_n^C(\tilde{\mathbf{X}}_n | H_k), \quad \forall k \in \mathbb{F}_K, \quad (2)$$

where  $\tilde{\mathbf{X}}$  denotes the sequence of random vectors  $\tilde{\mathbf{X}}_1, \dots, \tilde{\mathbf{X}}_N$ . In general, these observations are – similar to the observations  $X_1, \dots, X_N$  – not identically distributed, because of variation in distances  $d_n^C$  as well as that of the radiated powers  $P_n^C$ . Unlike the local decision rules, the global decision rule  $U_0 := \theta_0(\tilde{\mathbf{X}}_1, \dots, \tilde{\mathbf{X}}_N)$  depends on all observations in order to increase the overall classification probability.

All described assumptions are necessary in order to obtain an ideal framework suited for analyzing the power allocation problem without studying problems of different classification methods in specific systems and their settings.

### 2.1. Local classification rules

The local decision and classification rules  $\theta_n$  are mappings of the kind  $\theta_n: \mathbb{R} \rightarrow \mathbb{F}_K$ ,  $\forall n \in \mathbb{F}_N$ . In this work, hard-decision rules are used for performing local classification given by

$$\theta_n(X_n = x_n) = k, \text{ if } \tau_{n,k} < x_n \leq \tau_{n,k+1}, \quad k \in \mathbb{F}_K, \forall n \in \mathbb{F}_N, \quad (3)$$

where the thresholds  $\tau_{n,k} \in \mathbb{R}$  are suitably chosen. The thresholds must be calculated separately for every sensor node in order to perform optimal classification. They depend on the prior probabilities of the hypotheses. Their values can be calculated by a suboptimal approach which is described in Section 3.1. In this way, every sensor node has a local probability of correct decision given by

$$\text{Prob}(U_n = k | H_k) = \text{Prob}(\tau_{n,k} < X_n \leq \tau_{n,k+1} | H_k), \quad \forall k \in \mathbb{F}_K, \forall n \in \mathbb{F}_N \quad (4)$$

and a local probability of false decision given by

$$\text{Prob}(U_n \neq k | H_k) = 1 - \text{Prob}(U_n = k | H_k), \quad \forall k \in \mathbb{F}_K, \forall n \in \mathbb{F}_N. \quad (5)$$

### 2.2. Fusion of local decisions and the global classification rule

The local decisions  $U_1, \dots, U_N$  at the sensor nodes are conditionally independent due to uncorrelated and independent noisy communication channels. By applying the Bayesian-hypotheses-test criterion the optimal fusion rule at the fusion center is given by

$$U_0 = \theta_0(\tilde{\mathbf{X}} = \tilde{\mathbf{x}}) = \underset{k \in \mathbb{F}_K}{\text{argmax}} (\pi_k f^C(\tilde{\mathbf{x}} | H_k)), \quad (6)$$

where  $\pi_k := \text{Prob}(H_k)$  with  $\sum_{k=1}^K \pi_k = 1$  denotes the prior probability of hypothesis  $H_k$ . We use this formula to classify the target object. However, in order to optimize the allocation of the total power to the sensor nodes, we have to consider the overall classification probability. Therefore, we consider  $K$  pairwise disjoint regions  $\mathcal{R}_1, \dots, \mathcal{R}_K$  with

$$\mathcal{R}_k := \{\tilde{\mathbf{x}} \in \mathbb{R}^{K \times N} \mid \pi_k f^C(\tilde{\mathbf{x}} | H_k) \geq \pi_l f^C(\tilde{\mathbf{x}} | H_l), \forall l \in \mathbb{F}_K, l \neq k\}, \quad \forall k \in \mathbb{F}_K. \quad (7)$$

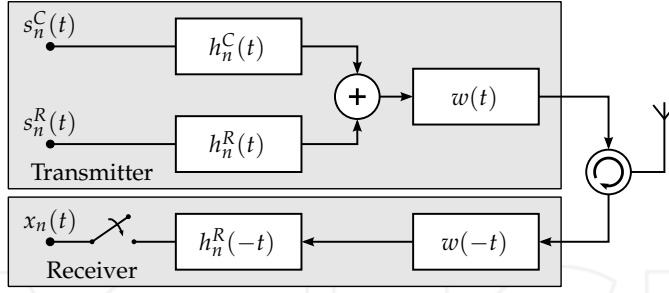


**Figure 2.** System model of the  $n^{\text{th}}$  sensor node with circulator and antenna.

According to [5], the expected value of correct classification is given by

$$P_c := \sum_{k=1}^K \text{Prob}(\tilde{\mathbf{x}} \in \mathcal{R}_k, H_k), \quad (8)$$

which in general cannot be analytically evaluated. Therefore, the previous formula cannot be used to optimize the allocation of the total power analytically. Consequently, we choose a different approach for the optimization, which is described in Section 3.3.

### 2.3. Ultra-wide bandwidth sensor nodes

In Figure 2 the system model of the considered impulse-radio UWB (IR-UWB) sensor nodes with pulse position modulation (PPM) is shown. The transmitter generates two streams of data symbols  $s_n^C(t)$  and  $s_n^R(t)$ .

The symbol stream  $s_n^C$  is used to transmit the local decisions  $u_n(i) \in \mathbb{F}_K$  at the time index  $i$  to the fusion center, which are generated by the algorithm defined in (3). We describe the data symbols by Dirac delta functions  $\delta(t - [u_n(i) - 1]\Delta)$ , which are shifted pulses on the time axis. Their alignment is determined by the modulation index  $\Delta$ . We assume that the product  $K\Delta$  is much smaller than the symbol duration. Thus  $K$  different data symbols can be transmitted to the fusion center. The transmission power  $P_n^C$  of this stream is variable in order to adjust transmission power and to enable distributed power allocation.

The symbol stream  $s_n^R$  establishes the radiation to the target object and uses always the same data symbol. Its transmission power  $P_n^R$  is also variable. In order to increase the available power range at every sensor node, time-division multiple-access (TDMA) method is used to separate both streams into different time slots and to periodically share the same power amplifier.

In order to eliminate collisions due to multiple access, each user stream is assigned to a distinctive time-shift pattern after passing through the blocks  $h_n^C(t)$  and  $h_n^R(t)$ . Their transfer functions are based on time-hopping sequences [13].

After superposition of both streams, a monocyclic pulse shape filter  $w(t)$  limits the bandwidth of the signal. This filter has to fulfill the Nyquist intersymbol interference (ISI) criterion in order to avoid the intersymbol interferences.

When this superposition is transmitted, a part of the radiated signal  $s_n^R$  will be reflected from the target surface back to the antenna. The received signal will pass through the matched-filter

$w(-t)$  and will be decoded from its time-hopping sequence by  $h_n^R(-t)$ . The additive noise signal  $b_n^R(t)$  will pass as well through both filters at the receiver. We denote the corresponding noise power by  $P_{\text{noise}}$ . If all receiver components are linear, then we can describe the received power by

$$\tilde{P}_{n|k}^R := P_n^R \frac{\alpha_n^R |r_k|^2}{g^2(2d_n^R)}, \quad \forall k \in \mathbb{F}_K, \forall n \in \mathbb{F}_N, \quad (9)$$

where the transmitted power is weighted by the product of the factors  $\alpha_n^R > 0$ ,  $|r_k|^2$ , and  $g^{-2}(2d_n^R)$ . The factor  $\alpha_n^R$  includes the radar cross section, the influence of the antenna, the impacts of the filters, and all additional attenuation of the transmitted power. Due to the reflection coefficient  $r_k$  of the target object the received power depends on the underlying hypothesis. The path loss function  $g$  depends on the assumed multipath propagation channel and is usually an increasing function of the distance between transmitter and receiver. Here, the factor of two in the distance results from that back and forth transmission between the transceiver and the object. The ratio of  $\tilde{P}_{n|k}^R$  and  $P_{\text{noise}}$  is the observed conditional SNR at the receiver and is given by

$$\gamma_{n|k}^R := \frac{P_n^R}{P_{\text{noise}}} \cdot \frac{\alpha_n^R |r_k|^2}{g^2(2d_n^R)}, \quad \forall k \in \mathbb{F}_K, \forall n \in \mathbb{F}_N. \quad (10)$$

Due to the Gaussian distribution of the noise, each sample is also a Gaussian random variable, which is conditionally distributed according to

$$f_n^R(X_n = x_n | H_k) := \frac{1}{\sqrt{2\pi P_{\text{noise}}}} \exp\left(-\frac{(x_n - \sqrt{\tilde{P}_{n|k}^R})^2}{2P_{\text{noise}}}\right), \quad \forall k \in \mathbb{F}_K, \forall n \in \mathbb{F}_N. \quad (11)$$

The local decision probabilities  $\text{Prob}(U_n = l | H_k)$ , see (4) and (5), can be computed by solving the integral

$$\begin{aligned} \tilde{\pi}_{n,l|k} &:= \text{Prob}(U_n = l | H_k) = \int_{\tau_{n,l}}^{\tau_{n,l+1}} f_n^R(x_n | H_k) dx_n \\ &= \frac{1}{2} \left[ \text{erf}\left(\frac{\sqrt{\tilde{P}_{n|k}^R} - \tau_{n,l}}{\sqrt{2P_{\text{noise}}}}\right) + \text{erf}\left(\frac{\tau_{n,l+1} - \sqrt{\tilde{P}_{n|k}^R}}{\sqrt{2P_{\text{noise}}}}\right) \right] \end{aligned} \quad (12)$$

for all  $k, l \in \mathbb{F}_K$  and for all  $n \in \mathbb{F}_N$ . Here, the mapping  $\text{erf}(z)$  denotes the error function of  $z$ .

#### 2.4. Fusion center

After radiation of the stream  $s_n^C$  by the sensor node  $S_n$ , the signal is attenuated depending on the distance and it reaches the antenna at the fusion center as depicted in Figure 3. The received signal is matched-filtered and decoded from its time-hopping sequence. Then a data splitter  $\mathbf{v}(t)$  is used to split the received signal into a  $K$ -dimensional vector space. This is necessary in order to retain the Euclidian distances between all transmitted symbols and achieve a higher classification probability. This filter is mathematically implemented as  $\sum_{k=1}^K \mathbf{e}_k \delta(t - (k-1)\Delta)$ , where  $\mathbf{e}_k$  is the standard basis vector of the  $K$ -dimensional space that points in the  $k^{\text{th}}$  direction. Therefore the received signals  $\tilde{\mathbf{X}}_1, \dots, \tilde{\mathbf{X}}_N \in \mathbb{R}^K$  are  $K$ -dimensional vectors. This new approach extends the method given by [13].

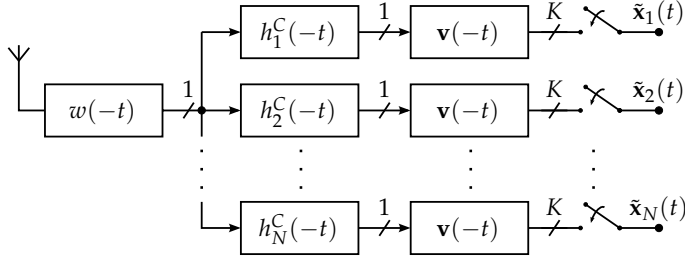


**Figure 3.** System model of the fusion center.

In case of additive zero-mean noise and due to the assumptions of  $w(t)$ , each vector sample of the received signal has the expected value of

$$\mathbf{m}_{n|l} := E(\tilde{\mathbf{X}}_n | U_n = l) = \sqrt{P_n^C \frac{\alpha_n^C}{g^2(d_n^C)}} \cdot \mathbf{e}_l, \forall l \in \mathbb{F}_K, \forall n \in \mathbb{F}_N, \quad (13)$$

which depends on the transmitted symbol  $U_n = l$ . Thus the received power from the  $n^{\text{th}}$  sensor node is given by

$$\tilde{P}_n^C := P_n^C \frac{\alpha_n^C}{g^2(d_n^C)}, \forall n \in \mathbb{F}_N, \quad (14)$$

where we assume that the path loss function is the same as for the first communication link. The power  $\tilde{P}_n^C$  is independent of the underlying hypothesis because the data stream  $s_n^C$  has the same power for all kinds of transmitted data symbols.

The additive noise signal  $b_n^C(t)$  will also pass through all the filters. We assume that the noise spectral density at the fusion center is the same as at the sensor nodes. Due to similarity in architecture of the fusion center and the sensor nodes, the noise power in each dimension of each stream is equal to  $P_{\text{noise}}$ . Because of the whiteness of noise, the interferences are uncorrelated in each dimension of each stream. Therefore the noise covariance matrix is determined by the product  $P_{\text{noise}} \cdot \mathbf{I}_K$ . Here  $\mathbf{I}_K$  denotes the identity matrix of size  $K$ .

Similar to (10) we define an observed SNR for each data stream at the fusion center and denote it by

$$\gamma_n^C := \frac{P_n^C}{P_{\text{noise}}} \cdot \frac{\alpha_n^C}{g^2(d_n^C)}, \quad \forall n \in \mathbb{F}_N. \quad (15)$$

Due to the Gaussian distribution of noise, each vector sample is a Gaussian random vector, which is conditionally distributed according to

$$f_n^C(\tilde{\mathbf{X}}_n | H_k) := \sum_{l=1}^K \frac{\tilde{\pi}_{n,l|k}}{(2\pi P_{\text{noise}})^{K/2}} \exp\left(-\frac{(\tilde{\mathbf{x}}_n - \mathbf{m}_{n|l})^T (\tilde{\mathbf{x}}_n - \mathbf{m}_{n|l})}{2P_{\text{noise}}}\right), \forall k \in \mathbb{F}_K, \forall n \in \mathbb{F}_N, \quad (16)$$

where the operator  $\mathbf{z}^T$  denotes the transpose of any vector  $\mathbf{z}$ .

Because of the convex superposition of multivariate Gaussian distributions, it is difficult to use (16) with the properties of (2) to optimize the distributed power allocation. Bounds, such as the Bhattacharyya bound [8], are also difficult to use due to multidimensional nature of (2) and (16). Therefore we propose an applicable technique which is motivated by concepts of information theory and is described in the next section.



### 3. Allocating power to the radar and to the communication task

In this section, we motivate and present an approach to suboptimally allocate transmission power to the radar and to the communication task. The objective is to maximize the overall classification probability, given a limited total transmission power  $P_{\text{tot}}$  that can be arbitrarily allocated to the radar task as well as to the communication task. A direct solution to this problem does not exist, since no analytical expression for the overall classification probability (8) is available. Instead, we independently maximize the mutual information of both communication channels to increase the information flow and in order to determine the power allocation. The motivation for this approach is the separation of the power allocation problem from the object classification procedure. Because in this case the data communication does not affect the classification of the target object.

Note that this theoretical concept is not realistic. However, we apply this concept as a heuristical method in this work.

#### 3.1. Threshold calculation

For the optimization of the thresholds in Section 2.1, in order to increase the overall classification probability, the analytic evaluation of (8) is needed. Due to the fact that this explicit form for the overall classification probability is unknown and due to the separation of the data communication from the classification task we propose the following simple approach to calculate the thresholds.

We increase the probability of correct decision of each sensor node independently to achieve suboptimal values for the thresholds. Thus, the overall classification probability should be increased as well. According to equations (4) and (12) the local probability of correct decision, which has to be maximized, is given by

$$\sum_{k=1}^K \text{Prob}(H_k) \text{Prob}(U_n = k | H_k) = \sum_{k=1}^K \frac{\pi_k}{2} \left[ \text{erf} \left( \frac{\sqrt{\bar{P}_{n|k}} - \tau_{n,k}}{\sqrt{2P_{\text{noise}}}} \right) + \text{erf} \left( \frac{\tau_{n,k+1} - \sqrt{\bar{P}_{n|k}}}{\sqrt{2P_{\text{noise}}}} \right) \right]. \quad (17)$$

Its solution can be found explicitly by using differential calculus. The corresponding result is identical to the one obtained by using the Bayesian-hypotheses-test criterion. It is given by

$$\tau_{n,k} = \begin{cases} \inf(\mathbb{I}_{n,k}) & \text{if } \mathbb{I}_{n,k} \neq \{\}, k \in \mathbb{F}_K, \\ \tau_{n,k+1} & \text{if } \mathbb{I}_{n,k} = \{\}, k \in \mathbb{F}_K, \\ \infty & \text{if } k = K + 1, \end{cases} \quad (18)$$

for all  $n \in \mathbb{F}_N$ , where the function  $\inf(\mathbb{I}_{n,k})$  is the infimum of the interval  $\mathbb{I}_{n,k}$  that is defined by

$$\mathbb{I}_{n,k} := \{x \in \mathbb{R} \mid \pi_k f_n^R(x | H_k) > \pi_l f_n^R(x | H_l), \forall l \in \mathbb{F}_K, l \neq k\}, \forall k \in \mathbb{F}_K, \forall n \in \mathbb{F}_N. \quad (19)$$

#### 3.2. Limitation of transmission power

We assume that both the radar and the communication signal use the same bandwidth and are uncorrelated to each other, due to separation of the sensing task and the communication task into different time slots (see Section 2.3). In this case and for each new classification process,

the limited total transmission power  $P_{\text{tot}}$  is an upper bound for the sum

$$\sum_{n=1}^N \underbrace{\underbrace{P_n^R}_{\text{Radar sensing}} + \underbrace{P_n^C}_{\text{Data communication}}}_{\text{Total transmission power of one sensor for a single observation}} \leq P_{\text{tot}}. \quad (20)$$

By using this restriction, we present the power allocation procedure in the next section. But, we will have a look at some special cases previously.

In real applications the transmission power of each sensor node is also limited. Consider the case in which all sensor nodes have the same power limitation  $P_{\text{max}}$  with  $\frac{P_{\text{tot}}}{N} \leq P_{\text{max}} < P_{\text{tot}}$ . If the power regulation, which is described in the next section, wants to allocate a higher power to  $P_n^R > P_n^C$  of the  $n^{\text{th}}$  sensor node than its limitation, then we set the transmission power  $P_n^R$  equal to its highest possible limitation given by  $P_{\text{max}}$ , recalculate  $P_n^C$  which is given in terms of  $P_n^R = P_{\text{max}}$ , discard this  $n^{\text{th}}$  sensor node from the list of unallocated sensor nodes, decrease the given total transmission power  $P_{\text{tot}}$  by  $P_{\text{max}} + P_n^C(P_{\text{max}})$ , and reallocate the remaining total power  $P_{\text{tot}} - P_{\text{max}} - P_n^C(P_{\text{max}})$  recursively to the remaining sensor nodes by the same procedure described in the next section. In a case, where the power  $P_n^C$  instead of  $P_n^R > P_n^C$  will be regulated higher than  $P_{\text{max}}$ , we can reverse the roles of both transmission powers and repeat this reallocation method until no more sensor nodes are left which exceed their power limitation. Therefore, the described limitation of the total transmission power is the generalized case which includes the limitation of the transmission power of each sensor node.

Note that this procedure is applicable for individual power constraints per node as well. Furthermore, note that in each iteration more than one node can be discarded from the list of unallocated sensor nodes in order to decrease the computation complexity.

### 3.3. Mutual information-based power allocation

For the maximization of the information flow we set the mutual information of both communication channels equal. This leads to the same symbol error probabilities on both sides for low SNR values. For each sensor node an upper bound for the mutual information of its first and second link can simply be calculated. The identity of obtained bounds

$$\frac{1}{2} \log \left[ 1 + \frac{P_n^R \alpha_n^R (|r_K| - |r_1|)^2}{4 P_{\text{noise}} g^2 (2d_n^R)} \right] = \frac{K}{2} \log \left[ 1 + \frac{P_n^C \alpha_n^C (K-1)}{P_{\text{noise}} g^2 (d_n^C) K^2} \right] \quad (21)$$

has to be computed in order to find the relationship between the powers for all  $n \in \mathbb{F}_N$ . After calculation and usage of the simple approximation

$$\sqrt[K]{1+x} \approx 1 + \frac{x}{K} \quad (22)$$

for any small values of  $x$  we obtain the analytical relationship

$$P_n^C = P_n^R \cdot \frac{\alpha_n^R}{\alpha_n^C} \cdot \frac{g^2(d_n^C)}{g^2(2d_n^R)} \cdot \frac{K}{K-1} \cdot \frac{(|r_K| - |r_1|)^2}{4}, \quad \forall n \in \mathbb{F}_N. \quad (23)$$

In the next step, we increase the overall information flow by maximization of the cumulative mutual information subject to the given total power of the sensor network. Then the

optimization problem is given by

$$\underset{P_1^R, \dots, P_N^R}{\text{maximize}} \quad \sum_{n=1}^N \frac{1}{2} \log \left[ 1 + \frac{P_n^R \alpha_n^R (|r_K| - |r_1|)^2}{4P_{\text{noise}} g^2(2d_n^R)} \right] \quad \text{subject to} \quad \sum_{n=1}^N P_n^C + P_n^R \leq P_{\text{tot}}. \quad (24)$$

It has to be considered that the sum of concave functions is also concave and that the arguments of the logarithms are linear functions of the powers. Furthermore, the domain of the feasible set is a closed convex set and, therefore, only one global maximum of the problem exists. This maximum can be explicitly calculated by using the method of Lagrange multipliers which is equivalent to the water-filling power allocation result [3]. The result is given by

$$P_n^R = P_{\text{noise}} \frac{g^2(2d_n^R)}{\alpha_n^R} \frac{4}{(|r_K| - |r_1|)^2} \cdot \max\left(0, \frac{\lambda}{\beta_n} - 1\right), \forall n \in \mathbb{F}_N, \quad (25)$$

where the factor  $\beta_n$  is defined by

$$\beta_n := \frac{g^2(2d_n^R)}{\alpha_n^R} \frac{4}{(|r_K| - |r_1|)^2} + \frac{g^2(d_n^C)}{\alpha_n^C} \frac{K}{K-1}, \forall n \in \mathbb{F}_N. \quad (26)$$

For the following equations, we assume that the factors  $\beta_n$  are ordered in an increasing manner. Then the water-filling level  $\lambda$  is a value specified by the inequality

$$\beta_{\tilde{N}} < \lambda \leq \frac{1}{\tilde{N}} \left[ \frac{P_{\text{tot}}}{P_{\text{noise}}} + \sum_{n=1}^{\tilde{N}} \beta_n \right], \quad (27)$$

where the number  $\tilde{N}$  with  $1 \leq \tilde{N} \leq N$  is a suitably chosen integer value for which the inequality

$$\sum_{n=1}^{\tilde{N}} (\beta_{\tilde{N}} - \beta_n) < \frac{P_{\text{tot}}}{P_{\text{noise}}} \quad (28)$$

holds. From (23) and (25) the allocated power for the second channel is determined as

$$P_n^C = P_{\text{noise}} \frac{g^2(d_n^C)}{\alpha_n^C} \frac{K}{K-1} \cdot \max\left(0, \frac{\lambda}{\beta_n} - 1\right), \forall n \in \mathbb{F}_N. \quad (29)$$

This allocation has the following interpretation. The sensor node  $S_n$  with the lowest  $\beta_n$  gets the largest part of the total power because its communication channels are possibly the best due to the low distances. Therefore the observation of the target object is less interfered by noise and consequently results in better data communication. Sensor nodes with higher distances get smaller parts of the total power and some of them do not get any power at all. The last ones participate neither in the data communication nor in the classification of the target object. Their information reliability is too poor to be considered for data fusion. More and more sensor nodes will become active by increasing the total power. Then the overall classification probability increases because more correct information is provided by the observations.

Note that we have used the approximation (22) in order to simplify the maximization problem and to find analytical solutions for all equations. Without any approximation the maximization problem yields the *Lambert's trinomial equation*, which still does not have any analytical solutions. Although the above approximation is only valid for low transmission

powers, we use the same solution for high transmission powers, too. If instead another approximation is used, the results are indeed different, but the behavior of solutions remains generally valid. However, this study is not the subject of this work.

### 3.4. Computational effort

In order to calculate the transmission powers (25) and (29) the computation of  $\beta_n$ ,  $\lambda$ , and  $\tilde{N}$  is necessary. The parameters  $K$ ,  $N$ ,  $P_{\text{tot}}$ ,  $P_{\text{noise}}$ ,  $r_k$ ,  $a_n^R$ , and  $a_n^C$  are fixed system parameters which are known to the computation unit. The distances  $d_n^R$  and  $d_n^C$  depend on the position of the target object and are therefore unknown. They can be estimated for example by a tracking algorithm. If these values are also determined, then the equations (25) to (29) can be calculated with little effort, because of simple mathematical operations such as summation and multiplication. The only difficulty is the evaluation of the path loss function  $g$ , which can include complex mathematical operations. Its complexity depends on the given multipath channel.

However, the computation effort of the equations (25) to (29) is less complex than the evaluation of the classification algorithm such as (6). If one can find simpler algorithms than (6) (see, for example [12]), then the assessment of the calculation effort becomes important and should be considered in detail.

## 4. Numerical results and conclusions

In this section we present some numerical results obtained by applying the proposed optimization method from Section 3. We simulate target objects with equal prior probabilities  $\pi_k = \frac{1}{K} \forall k \in \mathbb{F}_K$  in sensor networks with different settings as described in Section 2. In all results, we consider three different kinds of target objects with reflection coefficients chosen as  $|r_1| = 0$ ,  $|r_2| = \frac{1}{2}$ , and  $|r_3| = 1$ . Furthermore, the path loss function is modeled as line-of-sight propagation. The ratio  $\text{SNR} = 10\text{dB} \log\left(\frac{P_{\text{tot}}}{P_{\text{noise}}}\right)$ , instead of *received* SNRs, is depicted on the abscissa of all figures.

The verification of the proposed power allocation between both communication links of a single sensor node is shown in Figure 4. The overall error probability of the classification increases for higher SNR values for the case where the allocated power of one link is reduced by 10% and at the same time the power of the other link is stepped up by this 10%. When we reallocate a power amount of 10% – 30% to both links in an inverse manner, then the classification probability remains almost valid. This result shows that the proposed method allocates the given total power nearly optimal to both communication links, especially for higher SNR values.

In Figure 5 another verification of the proposed power allocation is shown, where a network of two sensor nodes is considered. The overall error probability of the classification decreases if we decrease the allocated power of the sensor node, which has the smallest part of the total power, by 10% and allocate this amount of power to the other sensor node. This result shows that the proposed method assigns the given total power suboptimal to the sensor nodes. The curves disperse, because of the approximation (22) which has been used for the equation (23).

As shown in Figure 6 the proposed method yields a better classification probability in comparison to a uniform power allocation where a network of ten sensor nodes is considered.

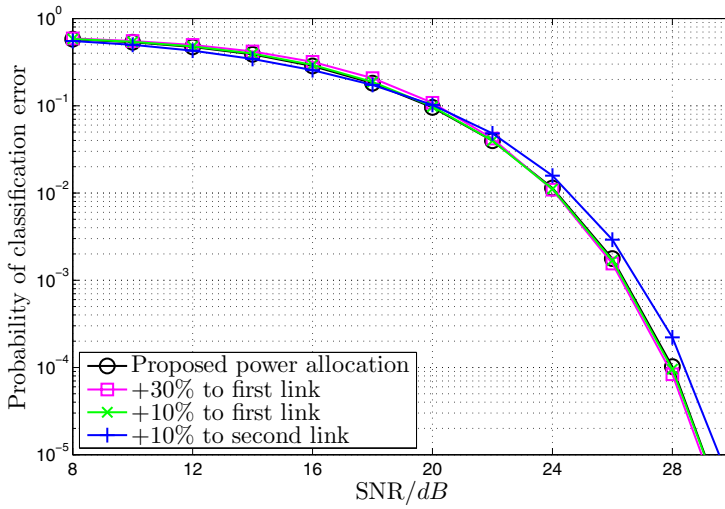


**Figure 4.** Verification of proposed power allocation between the two communication links of a single sensor node network.

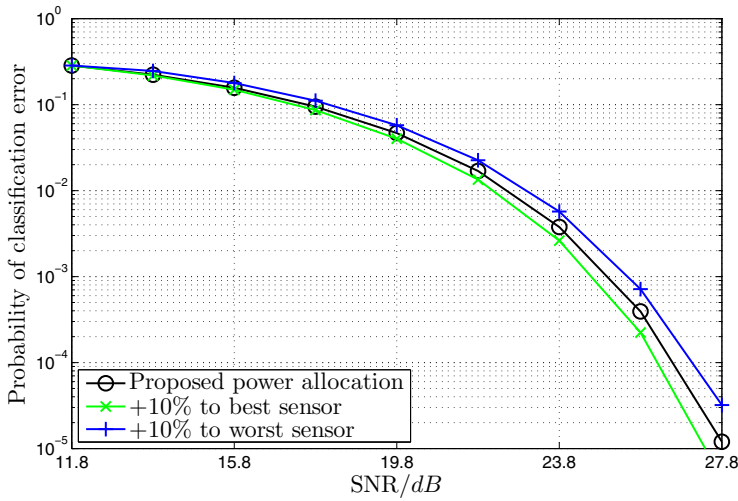


**Figure 5.** Verification of proposed power allocation between two sensor nodes.

In particular, it is shown that the same overall classification probability can be achieved with much lower transmission power, especially for low SNR values, by using an efficient power allocation method. Furthermore, the symbol-error probability of the sensor node with the highest part of the total power is also shown. The classification accuracy is better than the best symbol-error probability for higher SNR values, which affirms the gain of data fusion and illustrates the feasibility of object classification in this kind of distributed sensor networks.

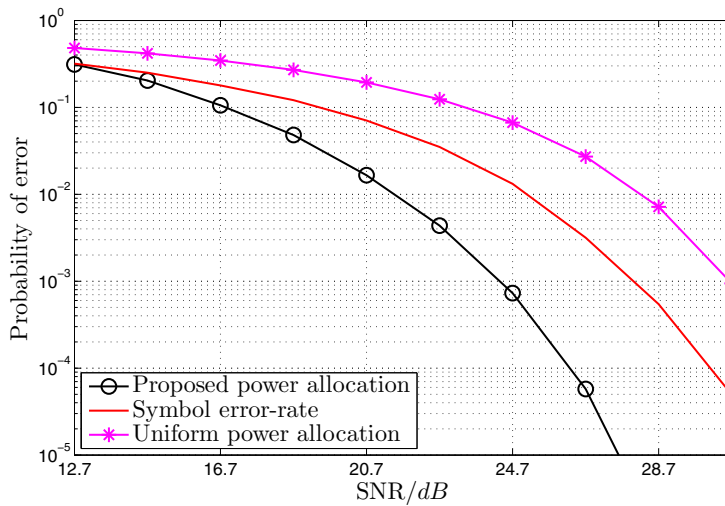


**Figure 6.** Comparison of proposed power allocation to a uniform power allocation in a network of ten sensor nodes.

## Author details

Gholamreza Alirezaei, Rudolf Mathar and Daniel Bielefeld

*Institute for Theoretical Information Technology, RWTH Aachen University, D-52056 Aachen, Germany*

## 5. References

- [1] Alirezaei, G. [2012]. Channel capacity related power allocation for ultra-wide bandwidth sensor networks with application in object detection, *IEEE ICUWB 2012 - International Conference on Ultra-Wideband*, Syracuse, NY, USA.
- [2] Bielefeld, D., Fabek, G., Zivkovic, M. & Mathar, R. [2010]. Optimization of cooperative spectrum sensing and implementation on software defined radios, *Proc. Int. Workshop Cogn. Radio Advanced Spectr. Management CogART*, pp. 1–5.
- [3] Cover, T. M. & Thomas, J. A. [2006]. *Elements of Information Theory*, 2nd edn, John Wiley & Sons, Inc.
- [4] Debes, C., Riedler, J., Zoubir, A. M. & Amin, M. G. [2010]. Adaptive target detection with application to through-the-wall radar imaging, *IEEE Trans. Signal Process.* Vol. 58(No. 11): 5572–5583.
- [5] Duda, R. O., Hart, P. E. & Stork, D. G. [2000]. *Pattern Classification*, 2nd edn, John Wiley & Sons, Inc.
- [6] Gezici, S., Tian, Z., Giannakis, G. B., Kobayashi, H., Molisch, A. F., Poor, H. V. & Sahinoglu, Z. [2005]. Localization via ultra-wideband radios: A look at positioning aspects for future sensor networks, *IEEE Signal Process. Mag.* Vol. 22: 70–84.
- [7] Hume, A. L. & Baker, C. J. [2001]. Netted radar sensing, *Proc. IEEE Int. Radar Conf.*, pp. 23–26.
- [8] Lapidith, A. [2009]. *A Foundation in Digital Communication*, Cambridge University Press.

- [9] Pescosolido, L., Barbarossa, S. & Scutari, G. [2008]. Radar sensor networks with distributed detection capabilities, *Proc. IEEE Int. Radar Conf.*, pp. 1–6.
- [10] Srinivasan, R. [1986]. Distributed radar detection theory, *IEE Proceedings-F* Vol. 133(No. 1): 55–60.
- [11] Surender, S. C. & Narayanan, R. M. [2011]. Uwb noise-ofdm netted radar: Physical layer design and analysis, *IEEE Trans. Aerosp. Electron. Syst.* Vol. 47(No. 2): 1380–1400.
- [12] Varshney, P. K. [1997]. *Distributed Detection and Data Fusion*, 1st edn, Springer-Verlag
- [13] Win, M. Z. & Scholtz, R. A. [2000]. Ultra-wide bandwidth time-hopping spread-spectrum impulse radio for wireless multiple-access communications, *IEEE Trans. on Communications* Vol. 48(No. 4): 679–691.
- [14] Yang, Y., Blum, R. S. & Sadler, B. M. [2010]. Distributed energy-efficient scheduling for radar signal detection in sensor networks, *Proc. IEEE Int. Radar Conf.*, pp. 1094–1099.